Adometer: Push the Limit of Pedestrian Indoor Localization through Cooperation

Zhice Yang, Xiaojun Feng, *Student Member, IEEE,* Qian Zhang, *Fellow, IEEE*

Abstract—Existing work on indoor localization achieves accuracy by conducting site surveys or deploying additional infrastructures. In this paper, we study the feasibility to design a low cost scheme, which is based on pedestrian dead reckoning and free from these requirements. Our method targets the scenarios where there are a large number of pedestrians in the public places holding their mobile phones while walking. First, we make one key observation that positioning errors brought by different pedestrians are diverse and can be mutually compensated. Second, we leverage the acoustic communication ability in mobile phone to enable users to exchange their locations when they meet with each other within a short distance. The received location information is crowdsourced to get a better location estimate. Finally, we use extensive experiments to evaluate the proposed scheme; the experiments are conducted in a 3500 square-meter area with more than 18 hours (more than 100km) real walking traces. Results show that our method is able to reduce the median localization error to 4m when the user density of the area is more than 50/3500 per square-meter.

Index Terms—Mobile phone sensing, Indoor localization, Dead reckoning

1 Introduction

Although numerous efforts have been paid for the indoor localization related research, there are still quite some open issues. Direct localization, such as fingerprint based methods [1], [2], [3], [4], is a common approach. However, these methods usually require expensive site surveys, special infrastructures or centralized processing to obtain accurate results.

Pedestrian Dead Reckoning (PDR) [5], [6], [7], [8], [9] is another kind of localization approach orthogonal to direct localization. It does not measure the current location directly. Instead, it starts from a known initial point and then updates locations by adding up all the incremental displacements measured by sensors. Obviously, this is an infrastructure-free solution for indoor localization, without offering the coverage of APs or centralized servers. However, its iterative calculation property results in huge cumulative error with low-cost mobile sensors, and thus the measurment results require calibration from time to time [9].

Our key observation is that moving behaviors of different pedestrians are diverse. Suppose all the users are using PDR for positioning, the property of diversity ensures that errors in distance and direction differ across different users. We also notice that the number of pedestrians in public places, such as airport or market, is large. Their diverse measurement errors can be mutually canceled once properly combined.

- *Z. Yang, X. Feng and Q. Zhang are with Department of Computer Science and Engineering, Hong Kong University of Science and Technology, Hong Kong SAR, China.*

Based on such observation, we enable PDR indoor localization in mobile phones without any addtional infrustructure by crowdsourcing the results among multiple individuals. We design and implement Adometer, an abbreviation for Acoustic Pedometer. To use it, each user simply holds the phone in one hand while walking. Adometer obtains self-location estimate by performing PDR on mobile phone sensors. Multiple users exchange their own location estimates through the acoustic channel once they meet. Because the acoustic communication distance is limited, the received location estimates from other users are treated as estimates for the user's location at that exact moment. Adometer takes advantage of the error diversity to fuse the received estimates with its own estimate to get a better localization result.

To make the whole system work, there are two challenges to be addressed. The first is how to exchange locations (broadcasting while receiving broadcast) among multiple users in a short period of time only if they meet. None of the off-the-shelf communication methods meet this requirement. The second is how to make use of other pedestrians' location estimates to reduce localization error. A carefully designed method and analysis are needed to ensure the effectiveness and reliability.

Adometer addresses the two challenges by contributing in the following aspects:

(a) We design and implement an effective acoustic communication method to exchange location estimates among meeting pedestrians. The locations are encoded in sounds with different frequency peaks to enable broadcasting among multiple users.

(b) We conduct real experiments to study the error property of PDR among multiple pedestrians. We

 DOI: No. 10.1109/TMC.2014.2329855

prove that the average of the PDR estimates for the same location from several individuals provides a better estimate for that location. Adometer leverages this property and uses the Extended Kalman Filter to fully utilize the received estimates and its own PDR results.

(c) To evaluate the design, we collecte 1100 mins walking traces in a $3500m^2$ place. The simulation based on the real traces shows the average median localization error is about $4m$ when the pedestrian density of the area is more than $50/3500m^{-2}$.

The rest of this paper is organized as follows. The first part is the realted work in this area. Then, we introduce our experimental observations of the error diversity of PDR. Third, a brief overview of our method is presented. After that, detailed design are described. The evaluation of Adometer is in section 6. We conclude the paper in the last section.

i	Pedestrian i
μ_δ^i	Bias error of step length of i as a random variable
$\sigma_{\mu_\delta}^2$	The variance of μ_δ^i among all the pedestrians
μ_φ^i	Bias error of moving direction of i as a random variable
$\sigma_{\mu_\varphi}^2$	The variance of μ_φ^i among all the pedestrians
$L_{n^i}^i$	Location estimate of i in i's step n^i
L_n	Abbreviation for $L_{n^i}^i$
L_n^-	Location estimate before Kalman Filter at step n
M_n	The number of meeting pedestrians at step n
$\bar{L}_{M_n}$	The average of received locations
d_g	Side length of the grid
d_e	Location error of the current estimate
d_s	Sound propagation distance
rL_n	Real location at step n
I	Unit matrix
K_n P_n^- P_n	Temporary variables for Kalman Filter
Q_n	Error covariance matrix of the PDR measurement
R_n	Error covariance matrix of $\bar{L}_{M_n}$

TABLE 1
Notations in the Main Text

2 Related Work

2.1 Indoor Localization

Indoor localization has attracted tremendous interests recently. Here only those closely related to our design are listed.

Dead reckoning is widely used in inertial navigation. Traditional implementations [10] need high quality inertial sensors. PDR is the extension of dead reckoning idea in low-cost portable devices. It measures distance by counting steps and determines direction by compass. [8] implements a prototype on mobile phone for outdoor pedestrian localization. They use the curve of the street as constraint to calibrate PDR error. [6] proposes a method for indoor usage, which needs a special IMU to be mounted on the foot and a well-defined indoor map. Zee [5] and [11] need a map showing pathways and barriers. Obviously, such map is not easy to generate and some barriers can move. As shown in the following sections, Adometer requires a grid map. However, the generation and the alignment of the grid map are really of zero-effort. UnLoc [9] observes that unique sensor readings caused by direction changes in physical turns, WiFi SSIDs in different areas and magnetic field distortion in some location can be used as virtual landmarks to calibrate PDR errors. As the calibration method needs the knowledge of all the users, a centralized server is required. The decentralized operation of Adometer is free of any additional infrastructures and operates in a distributed way.

Another kind of indoor localization is to measure the location directly. The most popular approach is based on fingerprint. It obtains the current location by comparing the measured fingerprint with the site-surveyed or model-based fingerprint map. RF fingerprint [1] and other fingerprint spaces [3], [4], [12] are explored in the current literature. The time-consuming, labor-intensive, and time-varying-vulnerable site survey [13] is the main bottleneck for them. Adometer is based on PDR, so that it is free of any site survey. Another approach of direct localization obtains location by measuring the time of flight [14] or angle of arrival [15], [16]. These methods are usually based on APs or other infrastructures, while Adometer has no such constrains. Further more, PDR method is orthogonal to the direct methods, Adometer can be applied to corporate with those direct localization methods to improve the positioning accuracy.

2.2 Acoustic Ranging and Communication

Acoustic ranging is introduced in many mobile systems or sensor network designs [17], [18]. The technique appears in localization problems for mobile devices [2], [19] as well. Both of them are based on WiFi localization and use acoustic ranging to further improve accuracy. Adometer dose not rely on accurate ranging, and it only makes use of the property that sound propagation distance is short to roughly guarantee the communication distance.

Sound signal can also be a carrier for location information. Sound beacons [20] in a certain place naturally indicates a rough location for mobile phones that can detect. [21] use the same property to detect the approaching pedestrians and locations of the meeting peers are corrected by a central server. However, their work only gives a solution/evaluation for two meeting pedestrians. Admeter is design and evaluated for multi-user situation. Another work [7] uses this property to calibrate moving trace by setting up sound beacons in fixed locations. In their design, however,

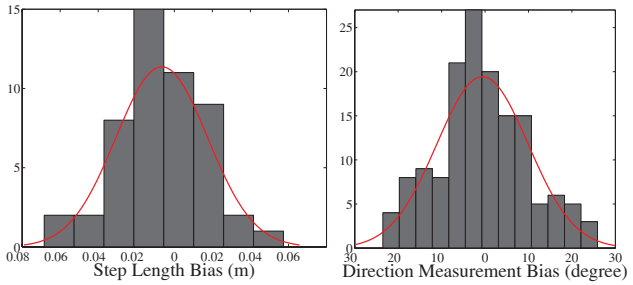

Fig. 1. Measurement Bias Distribution

a server is needed to help localization. In Adometer, locations are encoded into different frequency peaks to transmit locations among pedestrians. The process is finished in a distributed manner.

3 Observations

In this section, we study the error property of step length and moving direction measurement in PDR method, and then we derive the distribution of localization error among multiple participants through theoretical analysis.

In this paper, we based on the PDR method in [8]. It repetitively performs step detection and moving direction measurement. First, a learning-based approach is used to estimate an approximate step length in advance. The pedestrian walks for a certain distance, and the mobile phone counts the steps in the meantime. The distance can be measured by GPS outdoor or a tape indoor. The average step length in the learning process is used to estimate the step length for this person. As the step length of a pedestrian is pre-measured, the moving distance of the person is estimated by the counting steps. Second, the moving direction is obtained by the compass in the mobile phone. Finally, the displacement is obtained and added to the previous location to get the current location.

The localization error of PDR is determined by all the historical measurements. The error of each measurement consists of two parts: step length error and moving direction error. Two experiments are designed to study the properties of the two kinds of error respectively.

3.1 Step Length Measurement Error

In this subsection, we discuss the error distribution of step length measurement. We observe that the bias error of step length measurement is normally distributed among multiple users.

The pre-calculated step length is treated as user profile, thus only step detection is needed in the later calculation. This value contains bias error[1] if the pedestrian varies the walking intensity or the detection threshold is poorly selected.

We perform experiments to check the distribution of the bias error among different pedestrians. Ten volunteers are asked to walk along a $64.2m$ long corridor for ten times. The only instruction given to them is *"Please hold the phone in one hand"*. We get 100 accelerometer reading files (10 times per person) in total. The number of steps are counted and the average step length are calculated for each file. Therefore, ten step length values are obtained for each volunteer from his/her traces. For each volunteer, five of the ten values are selected and averaged to estimate his/her step length. The difference between the estimate of step length and the remaining five step length values is defined as the step length measurement bias μ_δ^i. μ_δ^i describes the major potion of the step length error in PDR measurement and is caused by factors such as inaccurate user profile (pre-calculated step length), false positive/negative step detection and so on. From those 100 files, we obtain 50 μ_δ^i. The histogram is shown in the left of Fig. 1.

The histogram shows a trend that the bias of step length among all the users is normally distributed. We perform *Lilliefors Test* on μ_δ^i to verify the hypothesis that they belong to a normal distribution family. The test returns p value. Small values of p casts doubt on the validity of the hypothesis. The test of μ_δ^i returns $p = 0.4927$, which means the distribution of the bias is close to a normal distribution. Note that the mean value of μ_δ^i is -0.0066. We perform *t-Test* on the hypothesis that this normal distribution is with 0 expectation. We get $p = 0.059$. From tests above, we experimentally verified that it is of low probability that the distribution of the bias dose not follow the distribution below:

$$\mu_\delta^i \sim N(0, \sigma_{\mu_\delta}^2). \tag{1}$$

3.2 Moving Direction Measurement Error

In this subsection, we discuss the error distribution of the moving direction measurement. We observe that the bias error of the direction measurement is normally distributed among multiple users.

The heading direction $\vec{H}$ of the mobile phone relative to the North $\vec{N}$ can be obtained from digital compass. The gap between $\vec{H}$ and the moving direction $\vec{M}$ of the pedestrian is how the user puts his phone. Fig. 2 shows the moving direction is undetermined even with accurate heading direction measurement.

In order to make the measurement less flexible while keeping the user burden minimal, we use the loose hint *"Please hold the phone in one hand"* to keep the moving direction roughly aligning to the heading direction of the mobile phone [2]. In section 7, we will

1. We focus on bias error rather than random error. As we put in the Appendix, random error is not a main error component in PDR. Intuitively, the randomness is averaged in the cumulative calculation.

2. The heading direction of the mobile phone is almost the moving direction of the pedestrian if the phone is held in one hand.

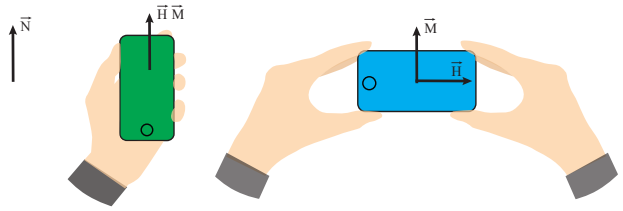

Fig. 2. Moving Direction Error Caused by the Holding Position. The mobile phone sensor can be used to measure the heading direction $\vec{H}$ of the phone with respect to the North $\vec{N}$. If $\vec{H}$ is aligned with the moving direction $\vec{M}$ (the green phone), the reading of the direction in the mobile phone indicates the walking direction of the pedestrian. On the contrary, the reading of the blue one says the West, even through the actual moving direction is the North. There is 90° bias error in the blue holding case.

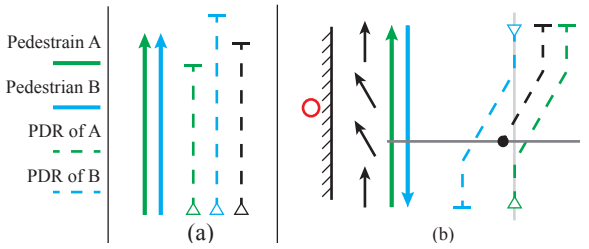

Fig. 3. Error Diversity Examples. In case (a), black dash is the average of their independent length estimates and is closer to the true location due to the error diversity of the length measurement. In case (b), the electromagnetic field (black arrows) is distorted by some source (red circle) and results in distortion in the PDR dash lines. A and B meet at the gray line and exchange their location estimates. The black dash is the new trace if A takes the average location(black point) as his location estimate after the meeting.

discuss more general cases without this restriction. Under such restriction, the error of moving direction is mainly caused by various *one hand* holding positions and environmental factors such as magnetic field deformation.

Again, we perform similar experiments to study the error distribution of the direction measurement. The corridors in our building are aligned to four geographic directions. When the pedestrian is moving in these corridors, the moving direction related to the North should be close to one of the four values: $0, \pi/2, \pi$ and $3\pi/2$. 8 volunteers participate in this experiment. 4 of them walk along a corridor in one direction and the remaining walk in the opposite direction. We record the heading direction of the mobile phone as the moving direction during the movement. We slice each direction-time sequence per second (about 2 steps) and average directions in each period to eliminate random error. The results are compared with known corridor directions. The difference μ_φ^i is the direction bias error in that sliced period. Finally, we obtain 146 μ_φ^i from 8 volunteers. The histogram is shown in the right of Fig. 1.

Similarly, we compare the distribution of the bias error of the direction measurement with the normal distribution. μ_φ^i scores $p = 0.3750$ in *Lilliefors Test* and $p = 0.4990$ in *t-Test*. These experiments show that

$$\mu_\varphi^i \sim N(0, \sigma_{\mu_\varphi}^2). \tag{2}$$

3.3 Localization Error of PDR

PDR takes step length and moving direction as input to calculate incremental displacement repetitively. The positioning error is determined by each independent measurement. Based on the experimental studies, we theoretically obtain the error distribution of PDR in the Appendix. In a nutshell, we prove that *the average of the pedestrian dead reckoning results of multiple individuals for a same location is a better estimate for that location compared with most individual measurement results*.

This claim is quite intuitive and guaranteed by the diversity of measurement error from multiple participants. While using the same PDR algorithm, some people have positive length/direction errors and some people have negative length/direction errors. When they average their estimates, errors are likely to be reduced. Fig. 3 gives two examples to illustrate why error (in length and angle) diversity can help positioning. Assume the moving direction $\vec{M}$ and the heading direction $\vec{H}$ of the phone are aligned. Solid arrows are their real moving traces and corresponding dash lines are their PDR estimates. Black dash are the average results, which are closer to the real location. Note that Fig. 3 gives only two simple examples to explain the motivation, a theoretical proof considering all the possible errors is presented in the Appendix.

4 Design Overview

In this section, we propose Adometer, whose design goal is to reduce the PDR error by leveraging the error diversity among multiple participants. Fig. 4 shows how it works. The boxes denote processing units while the non-box words denote the data flow. After the preparation step, Adometer repetitively performs three steps to update the new location.

In the preparation step, Adometer starts from an known initial location, such as the entrance. The location of this point can be determined by GPS or manually setup. All the Adometer users should share a same grid map to exchange locations. The grid map (Fig.5) is a real indoor map with virtual grids on it. Each grid has a number and represents a certain area. Adometer users use the number of the grid to indicate

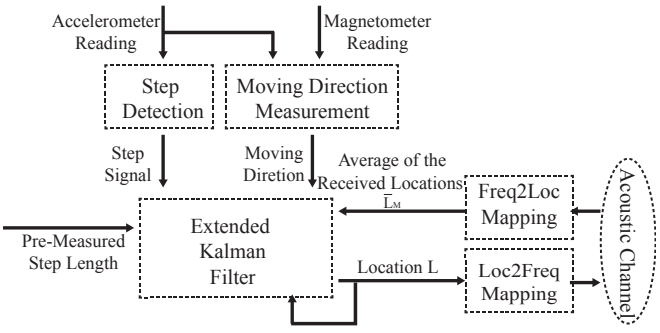

Fig. 4. Design Overview

the area under that grid. As long as the grid size is determined, it is trivial to cover an indoor map with grids.

In the first step, Adometer performs basic PDR [8]. The mobile phone detects the appearance of step while measuring its heading direction relative to the North from the sensor readings. An incremental displacement is calculated once a step is detected. User i's location estimate L_n^- is calculated through adding the displacement to his previous location L_{n-1}.

In the second step, different users exchange locations through acoustic channels. During the broadcasting process, Adometer of user i maps his location L_{n-1} to his map and looks up the corresponding grid area. The number of the grid is used to generate the corresponding acoustic frequency peak and broadcast through the speaker. At the same time, his microphone is continuously sensing frequency peaks from other users. The received peaks are re-mapped to locations $\{L_{n^j}^j\}$ of the center of the corresponding grids.

In the third step, Adometer uses Extend Kalman Filter to fuse L_n^- and $\{L_{n^j}^j\}$. Because the distance of sound propagation is limited, pedestrians that are able to communicate are restricted in a small area. Therefore, the measurement results from different users can be treated for the same location. Based on our observation, the average of the location estimates from multiple users in the same place can effectively reduce the estimate error. In this sense, the average of received locations $\bar{L}_{M_n} = \sum_{j=1}^{M_n} L_{n^j}^j / M_n$ is also an estimate for that location. An Extended Kalman filter is then used to fuse $\bar{L}_{M_n}$ and L_n^- to get a better estimate L_n for user i.

Adometer repeats the above three steps. L_n is treated as the previous location in the next processing cycle.

5 Adometer Localization Method

In this section, we describe the Adometer design in detail. We first introduce the acoustic communication which enables location exchange. Then we explain how to make use of the received information through Extended Kalman Filter.

5.1 Location Information Exchange

5.1.1 Design Goals

The communication method for Adometer should be able to (a) exchange locations among multiple users (b) in a short period of time (c) only if they meet (d) without any preexisting infrastructures.

5.1.2 Legacy Communication Methods

Before further discussion, it is necessary to check the limitation of existing communication methods in our unique scenario. There are five existing communication technologies on off-the-shelf mobile devices: 3G, WiFi, Bluetooth, FM and NFC.

We first eliminate FM, because it is illegal to generate FM signal in some countries or areas. NFC is not suitable because of its short communication distance (less than 20 cm). The communication target of 3G network is the cellular tower and it does not provide method to maintain the meeting constraint. The upper limit of the communication distance of WiFi and Bluetooth is designed for tens or hundreds of meters [3]. Such communication distance can not satisfy the tight meeting constraint. Moreover, their decentralized communication protocols suffer from cumbersome peering detection procedures[4]. Emerging WiFi Direct claims to improve this issue. However, we find a long peering time (a few seconds) between two mobile phones (Samsung Galaxy Note 2 and Galaxy S3), and this is not our unique observation [22]. The meeting time for two pedestrians can be as short as one second, thus long peering time would significantly reduce successful communication opportunities.

5.1.3 Acoustic Communication Design

The critical design goals cannot be achieved before we observe the two points below. (a) Sound propagation distance is short. (b) The amount of the information needed to describe the location for each user is not large. Specifically, the frequency of location change is slow (once per step or about $0.5s$) and accurate location description is not necessary. Modern mobile phone is able to sample and generate sound in a high frequency($16kHz$-$20kHz$ for Android) domain which is quiet compared with normal background noise [2], [19]. We can manipulate audio signal directly to design a simple and dedicated communication method for our scenario.

Adometer exchange locations in four steps: (a) It maps its own location estimate to a frequency peak, which corresponds to its nearest grid center. (b) It broadcasts a beacon with that frequency once a second. One second is divided into 20 slots. The broadcasting lasts for 2 successive slots which are

3. In some WiFi chip, the transmit power is adjustable for 20dB, which is still far from restricting range into meters.

4. Android does not support WiFi Ad-Hoc by default.

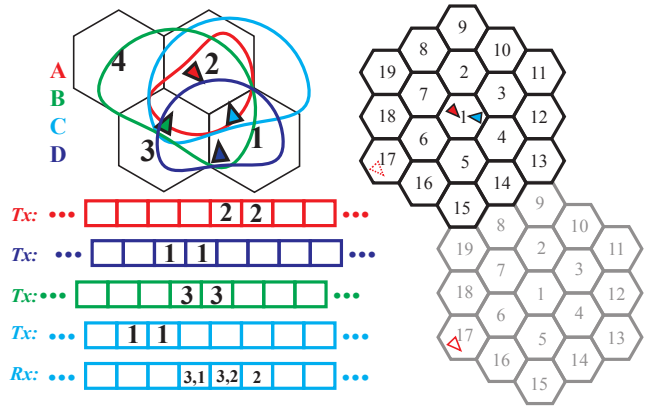

Fig. 5. Acoustic Communication Design. In the left, assume users transmit accurate location for simplicity. User C receives broadcasting from other users. If peaks are in different frequencies, they will not affect each other. If peaks are in a same frequency, they are randomly separated in the time dimension. The right part shows the location confusion caused by tiling. The self-estimate of the A is in grid 17(gray). If the grids size is too small, the receiver C may think the location of A is in grid 17(black).

randomly selected from those 20 slots. (c) Adometer is sensing peaks whenever it is not broadcasting. (d) The received frequency peaks are mapped to locations of the corresponding grid center. We explain the design below.

First, we use frequency domain peeks to carry information. Compared with the sound wave in time domain, the shape of the frequency wave doesn't change much during the propagation. A $20kHz$ peak wave in $1m$ is still a $20kHz$ peak wave in $5m$ even the peak magnitude decreases.

Second, we use pure sinusoid signals(peaks in the frequency domain) with certain frequency to represent an area. Because the self-location estimates are inaccurate, accurate coordinate description is unnecessary. However, the number of available peaks is limited by Doppler shift. Taking the speed of a pedestrian as $1m/s$, the maximum relative speed is $2m/s$. As the speed of the sound is about $340m/s$, the Doppler shift in frequency is about $\pm 120Hz$ if the peak is $20kHz$. We take $-50Hz$ to $+150Hz$ for each peak. This interval is asymmetric, because beacons with large negative shift (means they are walking away from each other) will be blocked by the body of the two pedestrians. Hence, the total available peaks are $(20k-16k)/200 = 20$. 19 grids are enough to generate a two level hexagonal grids coverage as Fig. 5. We can multiplex or tile 19 grids to cover any area or building[5]. Note that the alignment of the grids and the floor plan must be shared among all the users. This can be done by officially providing gridded floor plans on the web. As shown in Fig. 5, the tiling has a problem if the grid size is too small. The possible maximum error of the location estimate is d_e. The side length of each small grid is d_g. The sound propagation distance is d_s. Their relation is approximately given by[6] $d_g = (d_e + d_s)/3$. We take $d_g = 7m$ and $d_s = 3m$ based on experimental studies. As we will show in the Evaluation, there is no grid confusion since the maximum errors of most individuals are much less than $18m$ by using Adometer.

Third, Adometer needs to receive information from multiple pedestrians at the same time. In Fig. 5, each block is the time slot. We analysis frequency components in unit of one time slot. There are two problems, how long should one time slot be and how many slots should one beacon occupy. The time slot cannot be too short, otherwise the FFT resolution would not be enough. The time slot also should not be too long, otherwise Adometer may not have chance to distinguish different users in a same frequency. We take $0.05s$ for each time slot as a trade-off. For the second problem, if one broadcast beacon occupies too many slots, users broadcasting in the same frequency may not be distinguished. If the beacon is too short, the power of the beacon is too low to be separated from noise. Therefore, we take two time slots($0.1s$) as the beacon length. The receiver takes half of number of the detected beacons as an approximate estimate for the number of users in that peak frequency.

5.2 Extended Kalman Filter Design

Through the acoustic channel, a pedestrian receives location estimates from users met by him. In this section, we show how this information helps each individual reduce its localization error.

First, we consider the distribution of the average of the received locations. Pedestrian i moves through a location sequence $rL^i_{n^i}$. r means real location and n^i is the step number of i. We ignore the superscript of i for the Adometer host i that we examine. The dead reckoning gives an estimate of rL_n by L_n. For simplicity, we only consider the x-axis component of the location. Then the error in x_n is $e_{xn} = x_n - rx_n$. At some point, i encounters other pedestrians and receives their locations $\{x^j_{n^j}\}$, which is actually a set of locations of grid centers. $1 \le j \le M_n$. M_n is the number of pedestrian i met at step n. The average of the received locations is $\bar{x}_{M_n} = \sum_j x^j_{n^j}/M_n = \sum_j rx^j_{n^j}/M_n + \sum_j e^j_{n^j}/M_n$. The sound propagation ensures that those people are within a small distance,

5. First, treat the 19 black grids as a unit. Second, shift this unit as a whole to the nearby proper place as the gray one for example. Third, redu the second step until the map is covered by the grids.

6. In grids as Fig. 5, consider the situation where a Tx node is at the edge of grid 1. If a Rx node outside the surrounding 18 grids can hear the peak, there will be confusion. The minimum distance from the edge of of grid 1 to outside edge of those 19 grids is about $3d_g$

thus we have $\bar{x}_{M_n} \approx rx_n + \sum_j e_{n^j}^j / M_n = rx_n + \bar{e}_{xM_n}$. Based on the error diversity, we have proved in the Appendix (see the equation (8)) the average of the received $\{x_{n^j}^j\}$ is an estimate for the real location of user i, whose error is normally distributed and the expectation of the error is zero. We rewrite the equation here:

$$\bar{x}_{M_n} \approx rx_n + \bar{e}_{xM_n}, \bar{e}_{xM_n} \sim N(0, \sigma^2_{\bar{e}_{xM_n}}). \quad (3)$$

Second we consider the relation between the self dead reckoning estimate x_n and the received estimate $\bar{x}_{M_n}$. We view the pedestrian movement (rx_n) as a controlled process (x_n) governed by the stochastic(sensing error) difference equations. $\bar{x}_{M_n}$ provides direct state measurement for rx_n. To estimate rx_n, there is a trade-off between $\bar{x}_{M_n}$ and x_n. We use Kalman filter [23], which is naturally fitted in such scenario, to fully make use of both. We model the the walking process with stochastic difference equations:

$$rL_n = \begin{bmatrix} rx_n \\ ry_n \end{bmatrix} = \begin{bmatrix} rx_{n-1} + (l_{n-1} + \delta_{n-1})\cos(\theta_{n-1} + \varphi_{n-1}) \\ ry_{n-1} + (l_{n-1} + \delta_{n-1})\sin(\theta_{n-1} + \varphi_{n-1}) \end{bmatrix} = f(rL_{n-1}, u_{n-1}, w_{n-1}).$$

The received locations serve as an independent measurement:

$$z_n = \begin{bmatrix} \bar{x}_{M_n} \\ \bar{y}_{M_n} \end{bmatrix} = \begin{bmatrix} rx_n \\ ry_n \end{bmatrix} + \begin{bmatrix} \bar{e}_{xM_n} \\ \bar{e}_{yM_n} \end{bmatrix} = rL_n + v_n.$$

We use subscript n to denote the states in step n, thus $n-1$ is the previous step of n. l_n is the measured step length, which is a pre-measured constant. Its error is δ_n. θ_n is the measured counterclockwise angle between the moving direction and the East direction. φ_n is the angle error. rL_n is short for the current real location $[rx_n, ry_n]^T$. w_n is short for the sensing error vector $[\delta_n, \varphi_n]^T$. u_n is short for the dead reckoning measurement value $[l_n, \theta_n]^T$. The relation between them can be expressed in function $f(\cdot)$. Acoustic communication provides the location measurement z_n. Its measurement noise is $v_n = [\bar{e}_{xM_n}, \bar{e}_{yM_n}]^T$. From definitions above, the Kalman Filter algorithm tries to predict rL_n based on the knowledge of z_n. It falls into two steps running repetitively: *Predict step* and *Correct step*.

Predict step is responsible for projecting forward the current state and error covariance estimates to obtain the priori estimates for the next step:

$$L_n^- = f(L_{n-1}, u_{n-1}, 0), P_n^- = A_n P_{n-1} A_n^T + W_n Q_{n-1} W_n^T.$$

L_{n-1} is the estimate for rL_{n-1} given by the filter at step $n-1$. L_n^- is the priori estimate for rL_n. P_{n-1} is the posteriori estimate error covariance, which denotes the error variation of L_{n-1}. P_n^- is the error covariance matrix of L_n^-. A_n and W_n denote the linear relation among L_n^-, L_{n-1} and u_{n-1}, and it is obtained by the derivation on $f(\cdot)$. Q_n is the error covariance of w_n. σ_δ^2 and σ_φ^2 are the sensing error variance[7] of pedestrian i. These three matrices are listed here:

$$A_n = I, W_n = \begin{bmatrix} \cos\theta_n & -l_n \sin\theta_n \\ \sin\theta_n & l_n \cos\theta_n \end{bmatrix}, Q_n = \begin{bmatrix} \sigma_\delta^2 & 0 \\ 0 & \sigma_\varphi^2 \end{bmatrix}.$$

Correct step is responsible for incorporating measurement z_n into the priori estimate to obtain an improved posteriori estimate:

$$K_n = P_n^-(P_n^- + R_n)^{-1}, P_n = (I - K_n)P_n^-,$$
$$L_n = L_n^- + K_n(z_n - L_n^-).$$

R_n is the error covariance of v_n, which is defined in (3):

$$R_n = \begin{bmatrix} \sigma^2_{\bar{e}_{xM_n}} & 0 \\ 0 & \sigma^2_{\bar{e}_{yM_n}} \end{bmatrix}.$$

Finally, we obtain L_n as the estimate for rL_n. In practice, we take $P_0 = 0$ since the initial position is known. The pedestrian may not receive z_n every step. We simply let $K_n = 0$ in such situation, where L_n is totally determined by dead reckoning. Parameters in Q_n and R_n are discussed in Evaluation section.

6 Evaluation

We divide the evaluation into two parts. The first part validates the acoustic communication method, while the second part validates the overall Adometer localization performance.

6.1 Acoustic Communication

6.1.1 Communication Evaluation

We evaluate the feasibility of the acoustic communication in three situations.

The first part is stationary test. Two mobile phones (Samsung Galaxy S2 and Samsung Galaxy S3) are placed on three different corridors (our lab, outside of our lab, coffee shop) with different background noise levels (from 42dB to 51dB). One mobile phone is continuously sending increasing numbers from 0 to 19 (16kHz-19.8kHz) and the other is receiving. The volume of the speaker is set to 7. Once a number is received, both the false positive and false negative error can be derived (the increasing number pattern and the frequency are known). In the corridor of our lab, we also add two empty boxes between them to simulate the barriers in real situations (20cm in front of each mobile phone). The same experiment is repeated by varying the distances between two mobile phones. Since frequency domain is quiet [18], there is no false positive detection during the experiment. Therefore, the detection accuracy is defined as the number of detected peaks over the number of sent peaks. From

7. Different from (2) and (1), They come from the error distribution of a certain pedestrian. Note that (2) and (1) are the distribution of the bias error among multiple pedestrians.

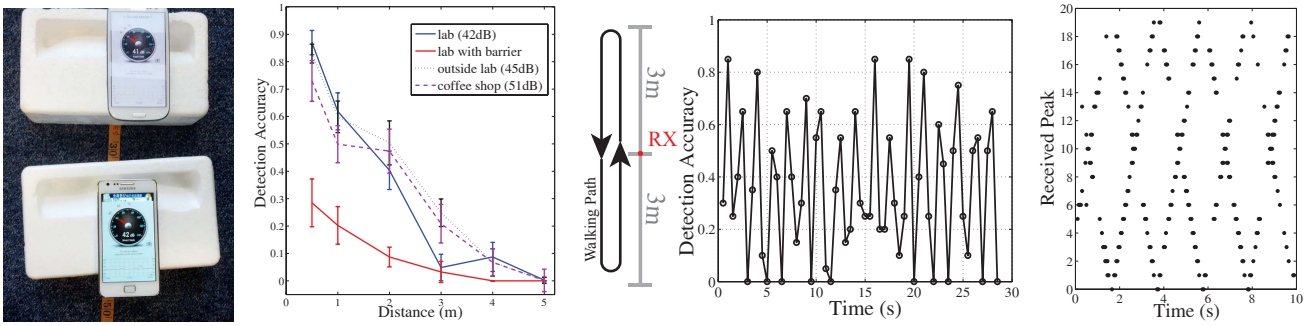

(a) Tools (b) Stationary Test (c) Moving Test (d) Multi Sender Test

Fig. 6. Acoustic Communication Evaluation

Fig. 6b, the effective communication distance is about $3m$. Curves of the receiving probability in different corridors are not exactly the same, but the trend is similar.

Second, we evaluate the feasibility when mobile phones are moving. The mobile phone setting is the same as the stationary test in our lab, but we hold one and move back and forth across a static one to simulate the situation where two pedestrians meet and leave each other. Fig. 6c shows a regular pattern. Due to the blocking of pedestrians' body, the detection accuracy decreases quickly when the moving one moves away from the static one. The test also shows that we do not need to worry about the Doppler Effect when two pedestrian move away from each other.

The third experiment simulates the multi-user situation. Two mobile phones are sending increasing numbers and receiving at the same time. A laptop is adjusted to a similar volume and sending decreasing numbers. The distance from one receiver to the two senders is $0.5m$ without barrier. Although the receiver cannot distinguish the source for the received peaks, the detected peak numbers of one mobile phones in Fig. 6d obviously show an increasing line and a decreasing line. The result indicates the success of receiving peaks from multiple senders simultaneously.

6.1.2 Power Consumption

A very important issue for acoustic communication in mobile device is the power consumption. In this section, we evaluate the energy consumed by the generation (Tx) and detection (Rx) of the acoustic signals[8]. The power is measured with the method in [25]. We connect a power meter to the Galaxy S2 to record the instant consumed power of the mobile phone.

The acoustic communication mainly has two components, the Tx part is used to generate frequency peaks that corresponding to the location. As the sin

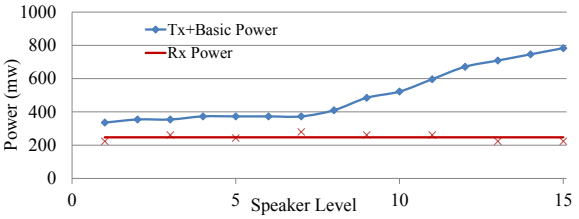

Fig. 7. Power Consumption

wave can be pre-stored in the mobile phone, the energy cost is similar to the audio play with the mobile phone speaker [26]. To measure the power, all the apps are closed except the acoustic communication. The screen is also turned off during the reading of the power meter. In order to get the upper bound of the power consumption of Tx, the mobile phone is set to play peaks in all the time intervals continually and without enabling Rx component. Results for different speaker levels are shown in Fig. 7. When the level of the speaker is low, the power of Tx is dominated by some basic operations (The OS overhead of media components, UI components and so on) of the audio play. The power is around 350mw, which is consistent with the result in [26]. When the level of the speaker is high, observable power is consumed in increasing the energy of the acoustic waves.

The second part of the acoustic communication is Rx, which is used to process the received acoustic signal to detect significant frequency peaks. The power of the Rx process is measured by subtracting the Tx power obtained in the previous paragraph from the total power of the acoustic communication with Tx and Rx on. As the Rx process is independent of the level of the speaker, the power of Rx is almost constant (≈247mw) across the x-axis of Fig. 7.

The result of the evaluation shows that the acoustic method has comparable power consumption with normal communication methods. Consider level 7 as the default speaker level, the maximum power consumed by the acoustic communication component is about 650mw. It is higher than Bluetooth (500mw)

8. Mobile Phone sensors also consume power in Adometer, but the amount [24] is not significant compared with that for communication.

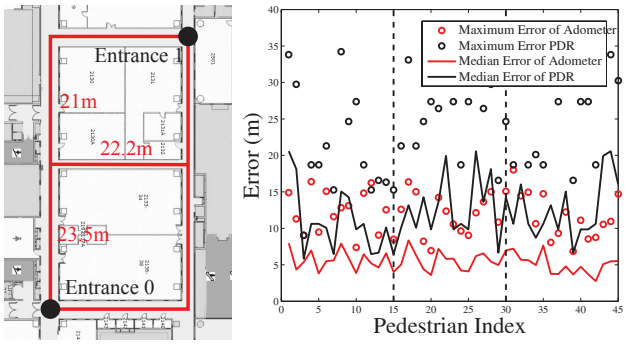

Fig. 8. Indoor Experiment

and less than making phone call (>700mw) and WiFi connections (>800mw) [26]. Moreover, the current FFT algorithm is implemented with look-up table of the trigonometric functions and is the main computational overhead of the Rx component. The power consumption can be further reduced by DSP ICs or Sparse FFT algorithm [27].

6.2 Real Trace Simulation

6.2.1 Methodology

As existing crowdsourcing work [7], [9] mentioned, it is difficult to deploy large scale experiment due to the limitation of sample size. Therefore, we adopt a real trace based simulation. The insight is that the real moving trace and the sensor readings of a certain pedestrian are determined no matter how the mobile phone gives location estimate. It motivates us to merge the traces collected from different periods and different volunteers to simulate multi-user walking in the same period.

One big issue is the ground truth. Due to the absence of GPS coverage in indoor environment, the real moving trace of a certain pedestrian is hard to obtain. Normally, the experimenter may ask volunteers to walk along predefined paths. We carry out such experiments in our academic building, but the scale is limited and well-defined paths cannot fully simulate real cases such as a modern shopping center. To address this concern, we design experiments in an outdoor football field, where the volunteers can walk freely. Importantly, we can gather GPS traces as the baseline to validate our design in more realistic situations.

A mobile phone application is running to gather sensor data. It continuously writes four-tuples <time, direction, GPS_{Long}, GPS_{Lat}> into the log file, which is then processed by a simulator that can simulate pedestrians' movement and mutual information exchange. The simulator takes sensing and GPS log to construct a virtual pedestrian. After joining the virtual area, each virtual pedestrian acts as its own log file. Each virtual pedestrian is able to perform Adometer algorithm with the input sensor data and the exchanged locations. They move along GPS traces, and can hear other pedestrians' beacons according to the probability measured in Fig. 6b. This simulator is used in the flowing evaluation experiments.

6.2.2 Experiments in Indoor Corridor

These experiments are performed in corridors with two circles. 4 volunteers are asked to hold a phone in one hand and walk in the area. The entrance is randomly selected and the direction is also randomly selected when they encounter turns. Each trace is $3mins$ and each volunteer collects 4 traces. The total number of traces is 16. The ground truth is collected by manually marking time at turns and transformed to simulator-compatible format. Since the ground truth gathering method cannot be applied to other corridor shapes, we limit the experimental scale in the indoor corridor and briefly give the results in Fig. 8. The mean of the median error of basic PDR is $12.1m$. The mean of the median and maximum error of Adometer is $5.4m$ and $12m$. The simulation settings are the same as the next part, in which we provide more details.

6.2.3 Experiments in Outdoor Football Field

Experiments in one half of a football field ($3500m^2$) are performed by 3 volunteers. We set 4 entrances at each side of the field. They are asked to walk randomly in the restricted area. The enter point and exit point are randomly selected from 4 entrances. Each trace lasts for 20 $mins$. We collected 55 traces in total, and the collection process takes us 3 weeks. The environmental condition is also diverse. We encounter different weather conditions (cloudy, rainy, sunning and typhoon) and temperatures during the data collection.

However, 55 traces are not sufficient to cover real conditions. In a real mall, some of the consumers are coming in while some of them are leaving. Except the opening and closing periods, the user density won't change dramatically. Therefore, the steady-state, where the number of pedestrians in this area keeps a dynamic equilibrium, is of great importance. If the walking time of each pedestrian is the same, the number of traces needed to reach the steady-state equals to the number of pedestrians in the steady-state. Hence, $55 * 3$ is the minimum requirement to study the performance of the Adometer. We extend the trace pool to 220 by reflecting along x-axis, y-axis and rotating 180 degrees.

The evaluation is performed in the simulator with default parameters obtained in the next part6.2.4. We randomly select 200 virtual pedestrians from the trace pool and add them to the virtual area one by one with the same time interval. The time interval is determined by the default user density.[9] Fig. 9b shows

9. By default, the time interval is $20min/50$ when the density is 50. They reach steady-state in the $50th$ pedestrian.

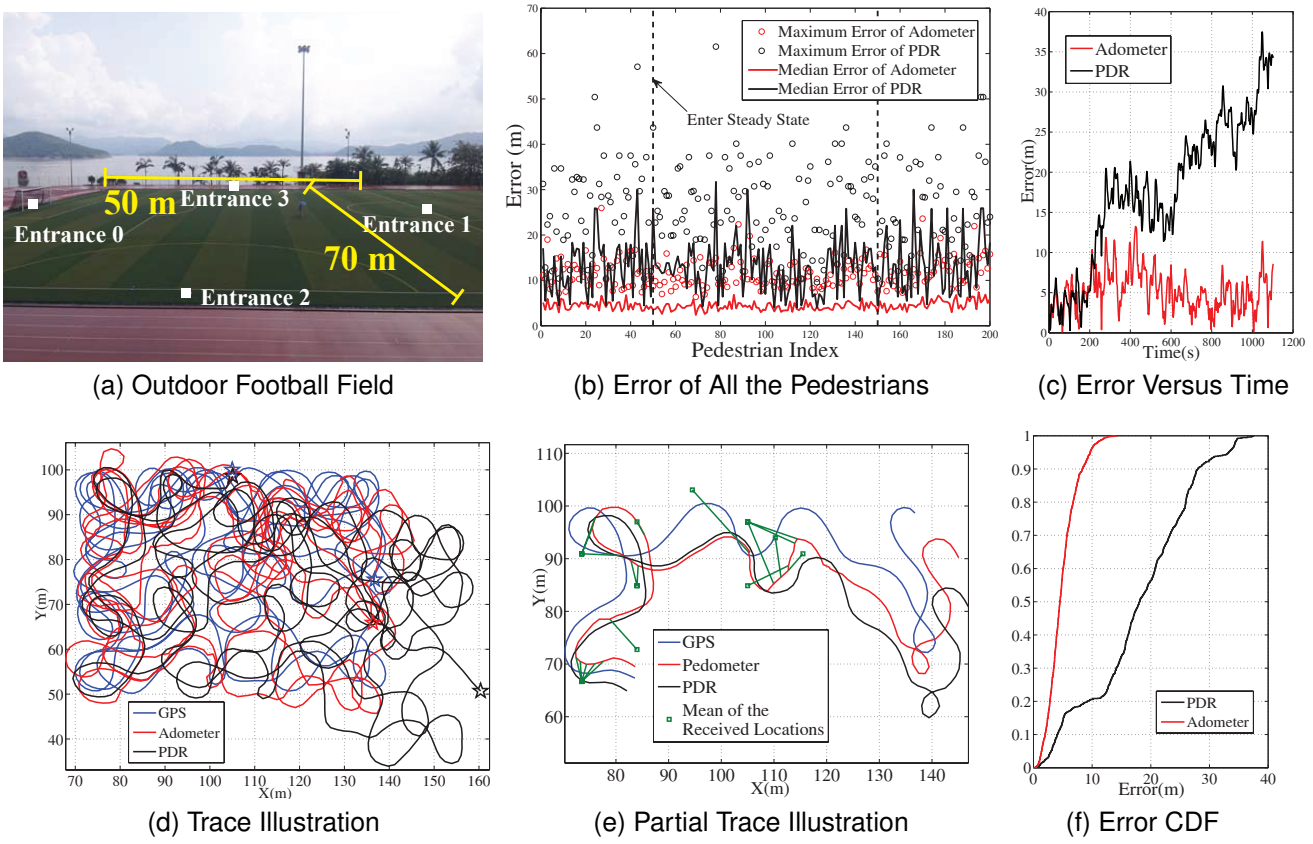

(a) Outdoor Football Field (b) Error of All the Pedestrians (c) Error Versus Time

(d) Trace Illustration (e) Partial Trace Illustration (f) Error CDF

Fig. 9. Outdoor Experiment. (a)(b) is overall results, (c)(d)(e)(f) are the results from one pedestrian.

the statistical localization error refer to GPS traces during the whole movement for each pedestrian. "PDR" means the pedestrian dead reckoning method without crowdsourcing, and it contains large error. Due to the restriction of the moving area, the error does not increase to larger values. Its average of the median error is $13m$. In Adometer, the average of the median error and maximum error is $4.4m$ and $11.7m$. Pedestrians between two dash lines are in the steady-state. Errors outside steady-state do not increase much, suggesting Adometer benefits all the participants in spite of their entering time.

Fig. 9c, 9f, 9d and 9e are taken from the same pedestrian in the center (index=101) of the simulation. Fig. 9f shows the error in Adometer is nearly uniformly distributed from zero to the maximum value. Hence the median error is close to the mean error. We also check other pedestrians. The black curves are different, but the red curves are almost identical. This indicates that the algorithm is stable and the error does not fluctuate much among different users. Fig. 9c shows the error does not increase with time and is bounded. Fig. 9d illustrates how Adometer helps each individual. The stars represent start points and end points of the traces. By comparing the difference between GPS and PDR, the fact shows their "shapes" are analogous during most of the time. The curve of PDR is distorted in some points and displacement inherits. Fig. 9e is a part of Fig. 9d. It shows how the estimates from other pedestrians help Adometer to avoid distortion. The green points are the average of the received locations (value of z in 5.2). Each green line represent one chance of successful receiving. It links one green point and the receiving location on the moving trace. Clearly when X is around 110m, the pure PDR result is pulled by the "force" of the green point (Kalman Filter takes the z value adjust the PDR measurement) to the GPS trace direction. The "force" is in the right direction, because of the fact we proved that the average of the received locations is a better estimate than that of the individual PDR.

6.2.4 *Parameter Selection*

The performance of Adometer depends on several parameters, and they are easy to set. The list of all the parameters is: (a) grid size d_g, (b) the error covariance matrix R of the average of received location estimates, (c) the error covariance matrix Q of the dead reckoning estimate, (d) user density and (e) sound propagation distance d_s. Since the average of the three experimental curves is used to determine the detection probability in6.2, evaluation for factors excluding d_s is shown in Fig. 10a, 10b, 10c and 10d. The value of each parameter is shown in the yellow

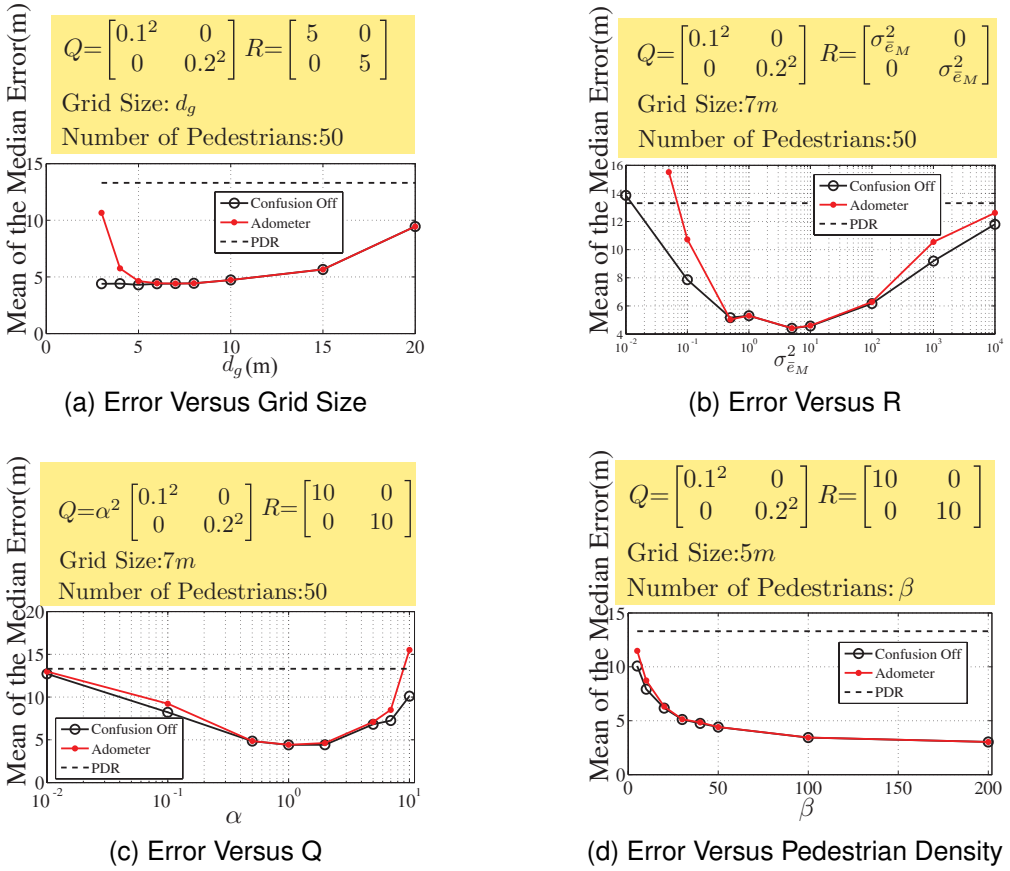

(a) Error Versus Grid Size

(b) Error Versus R

(c) Error Versus Q

(d) Error Versus Pedestrian Density

Fig. 10. Adometer Parameters

box over the curve. Users are randomly selected from the trace pool. The random seed is the same long int to ensure the same selection sequence across different parameters.

Grid size is defined as the side length of the hexagon. Its default value is set as $d_g = 7m$. To quantify the impact of the confusion problem in the early discussion5.1.3, two modes are supported in the simulator. *confusion on* is the real situation. In *confusion off*, virtual users map peaks to locations without confusion. From Fig. 10a, the confusion affects the performance of Adometer when the grid size is less than $6m$. This is because the maximum error of Adometer exceeds the safe distance, thus pedestrians mutually provide usefulness or even wrong estimates. However, the error of the Adometer is not sensitive to the increase of d_g. It is easy to adopt a conservative choice with larger grid size than the optimal.

R is determined by the error variance of the average of the received location estimates. Its approximate distribution is proved in (8), but its parameters are unknown. The basic properties of grids give us an intuition. Even though an estimate of a location is accurate, its value is blurred by mapping to the grid center. Thus the magnitude of the variance of each estimate should be around the magnitude of the variance of uniform distribution in one grid(take grid size 7, the variance is 16). Fig. 10b shows what we proposed. The error does not change much when the variance is between 1 and 100, meaning that the value of R is quite flexible. $R = 5I$ is set as default value. The figure also shows the effectiveness of the Kalman filter. When R is small, Adometer takes the average value of the received locations directly as its estimate, which is far from the optimal. When R is very large, Adometer takes PDR as its estimate and the curve shows the error is close to the PDR line.

Q is determined by the variance of the step length and angle measurement error w_n. For one individual, $E(w_n)$ is not necessarily 0 and the bias is unknown. We choose $\sigma_{\delta_n} = 0.1$ and $\sigma_{\varphi_n} = 0.2$ as the default value based on the experiments in Observations section to ensure that the variance is large enough to contain the bias. The evaluation results show that these values are reasonable. The curve also shows that the error of Adometer does not change much with rational Q values. The increase or decrease of Q goes in the opposite direction compared to R. Adometer tends to believe the dead reckoning results if Q is small and vice versa.

The number of pedestrians is used to represent the user density, because the experimental field is a fixed area. The default density is 50 (50/3500 person per m^2). In a real indoor situation, the user density in the

available areas, such as corridors, is much higher. As the football field in our experiment is $3500m^2$, each users occupies about $70m^2$. If a corridor is with 2m width, the density is 35m per person. Such a density is very low in indoor situations such as campus buildings, stations, malls and so on. In Fig. 10d, the accuracy does not increase much when the density exceeds [10] 50. The baseline error (GPS) and the grid size are consider to be the main limitation in high density situations. Moreover, errors are reduced when there are only 5 people walking at the same time, meaning that Adometer benefits users even when the density is very low.

7 Discussion

The basis of Adometer algorithm is the diversity of the received location error. Therefore, the effectiveness of the Adometer depends on how many locations it received and the diversity of the error in received locations.

In scenarios on which the paper focus, such as the market and campus, there are enough pedestrians, but it is possible that the user does not receive any locations for a period of time and his location error exceeds the grid confusion bound (18m according to section 5.1.3). At this time, the reader may think the user's estimate contributes negatively for other users and can not benefit from other users. However, this is not the fact in real scenarios. In Fig. 9b, several red circles are larger than 18m and the maximum one is about 27m. After removing those users, we find there is no concrete increase in the average of the location error. There are two reasons for the result. First, the location exchange process is something like averaging, so that the average result is dominated by the majority. Second, the moving area of a pedestrian is limited, and the error of the random walk of the pedestrian is also limited. Therefore, it is possible that the error larger than the confusion bound decreases below to the confusion bound at some time occasionally. After that, the pedestrian will again benefit from Adometer.

In some special floor plans that violate diversity by restricting the movement of pedestrians in a certain direction (For example, some one-way paths in subway station), Adometer can work with other method to improve its accuracy.

Another possible concern for current implementation lies on the experimental requirement on holding the mobile phone *in one hand*, which is used to keep the relative position between the pedestrian and the mobile phone stable. If the mobile phone is located in other locations such as pocket, Adometer requires an initial process to train and get the relative position with respect to the pedestrian. As there are existing solutions [5], [9], [21] for getting the this relation, the related techniques are out of the scope of this paper. However, we view a more complete implementation as a part of our future work.

10. 800 virtual pedestrians are selected to perform 200 density experiment and 400 for 100 density experiment. All the other experiments in our evaluation are performed by randomly selecting 200 virtual pedestrians except this one, because more virtual users are needed to fill in the area when the density is larger than 50.

8 Conclusion

By utilizing the diversity of error in multiuser measurement, we design and implement Adometer, a method cooperatively reduces the error in pedestrian dead reckoning. Pedestrians that can hear each other exchange their location estimates through acoustic channel, and the received locations are incorporated by Kalman filter to improve the individual measurement results. We validate this design by conducting thorough evaluation. It achieves median localization error as low as 4m without any preexisting infrastructures. Moreover, the design of Adometer is orthogonal to most of the existing indoor localization approaches; it is promising to explore the combination to get more robust and practical solutions for indoor localization.

References

[1] K. Chintalapudi, A. Padmanabha Iyer, and V. N. Padmanabhan, "Indoor localization without the pain," in *MobiCom*, 2010.

[2] H. Liu, Y. Gan, J. Yang, S. Sidhom, Y. Wang, Y. Chen, and F. Ye, "Push the limit of WiFi based localization for smartphones," in *MobiCom*, 2012.

[3] J. Chung, M. Donahoe, C. Schmandt, I.-J. Kim, P. Razavai, and M. Wiseman, "Indoor location sensing using geo-magnetism," in *MobiSys*, 2011.

[4] Y. Chen, D. Lymberopoulos, J. Liu, and B. Priyantha, "FM-based indoor localization," in *MobiSys*, 2012.

[5] A. Rai, K. K. Chintalapudi, V. N. Padmanabhan, and R. Sen, "Zee: zero-effort crowdsourcing for indoor localization," in *MobiCom*, 2012.

[6] O. Woodman and R. Harle, "Pedestrian localisation for indoor environments," in *UbiComp*, 2008.

[7] I. Constandache, X. Bao, M. Azizyan, and R. R. Choudhury, "Did you see bob?: human localization using mobile phones," in *MobiCom*, 2010.

[8] I. Constandache, R. Choudhury, and I. Rhee, "Towards mobile phone localization without war-driving," in *INFOCOM*, 2010.

[9] H. Wang, S. Sen, A. Elgohary, M. Farid, M. Youssef, and R. R. Choudhury, "No need to war-drive: unsupervised indoor localization," in *MobiSys*, 2012.

[10] D. Titterton, J. Weston, D. H. Titterton, and J. L. Weston, *Strapdown Inertial Navigation Technology, 2nd Edition*. IET, 2004.

[11] F. Li, C. Zhao, G. Ding, J. Gong, C. Liu, and F. Zhao, "A reliable and accurate indoor localization method using phone inertial sensors," in *UbiComp*, 2012.

[12] S. P. Tarzia, P. A. Dinda, R. P. Dick, and G. Memik, "Indoor localization without infrastructure using the acoustic background spectrum," in *Mobisys*, 2011.

[13] Z. Yang, C. Wu, and Y. Liu, "Locating in fingerprint space: wireless indoor localization with little human intervention," in *MobiCom*, 2012.

[14] D. Giustiniano and S. Mangold, "CAESAR: carrier sense-based ranging in off-the-shelf 802.11 wireless LAN," in *CoNEXT*, 2011.

[15] S. Sen, R. R. Choudhury, and S. Nelakuditi, "SpinLoc: spin once to know your location," in *HotMobile*, 2012.

[16] J. Xiong and K. Jamieson, "Towards fine-grained radio-based indoor location," in *HotMobile*, 2012.

[17] C. Peng, G. Shen, Y. Zhang, Y. Li, and K. Tan, "BeepBeep: a high accuracy acoustic ranging system using COTS mobile devices," in *SenSys*, 2007.

[18] J. Yang, S. Sidhom, G. Chandrasekaran, T. Vu, H. Liu, N. Cecan, Y. Chen, M. Gruteser, and R. P. Martin, "Detecting driver phone use leveraging car speakers," in *MobiCom*, 2011.
[19] R. Nandakumar, K. K. Chintalapudi, and V. N. Padmanabhan, "Centaur: locating devices in an office environment," in *MobiCom*, 2012.
[20] N. B. Priyantha, A. Chakraborty, and H. Balakrishnan, "The cricket location-support system," in *MobiCom*, 2000.
[21] Y.-T. Li, G. Chen, and M.-T. Sun, "An indoor collaborative pedestrian dead reckoning system," in *Parallel Processing (ICPP), 2013 42nd International Conference on*. IEEE.
[22] "Wifi direct links: http://www.youtube.com/watch?v=RM3Q1oiHTGU http://www.youtube.com/watch?v=gCEawDprnOQ."
[23] G. Welch and G. Bishop, "An introduction to the kalman filter," 2006. [Online]. Available: http://www.cs.unc.edu/~welch/media/pdf/kalman_intro.pdf
[24] B. Priyantha, D. Lymberopoulos, and J. Liu, "Littlerock: Enabling energy-efficient continuous sensing on mobile phones," *Pervasive Computing, IEEE*, vol. 10, no. 2, 2011.
[25] R. Mittal, A. Kansal, and R. Chandra, "Empowering developers to estimate app energy consumption," in *Mobicom*, 2012.
[26] A. Carroll and G. Heiser, "An analysis of power consumption in a smartphone," in *USENIX ATC*, 2010.
[27] H. Hassanieh, L. Shi, O. Abari, E. Hamed, and D. Katabi, "Ghz-wide sensing and decoding using the sparse fourier transform," in *Infocom*, 2014.

APPENDIX

In this section, we prove the location error distribution property.

We use $x^i_{k^i}$ to denote x component of the dead reckoning location $L^i_{k^i}$ of pedestrian i at step k^i. Its step length is $l^i_{k^i}$, moving direction is $\theta^i_{k^i}$. If the initial location is x^i_0, the real location at step n^i is given by $x^i_{n^i} = x^i_0 + \sum_{k^i=1}^{n^i} l^i_{k^i} \cos\theta^i_{k^i}$.

The measurement performed by dead reckoning introduces two kinds of error, step length error $\delta^i_{k^i}$ and and direction error $\varphi^i_{k^i}$. Thus the location error at step n^i is:

$$\begin{aligned} e^i_{n^i} &= x^i_{n^i} - r x^i_{n^i} \\ &= x^i_{n^i} - (x^i_0 + \sum_{k^i=1}^{n^i} (l^i_{k^i} + \delta^i_{k^i}) \cos(\theta^i_{k^i} + \varphi^i_{k^i})) \\ &\approx \sum_{k^i=1}^{n^i} (\varphi^i_{k^i} l^i_{k^i} \sin\theta^i_{k^i} - \delta^i_{k^i} \cos\theta^i_{k^i}). \end{aligned} \tag{4}$$

We view the measurement in a period, in which the statistical properties of the error do not change much. Then, all the $\delta^i_{k^i}$ are independent and identically distributed (i.i.d.). Step length error has two parts. The system error $\mu^i_\delta = E(\delta^i_{k^i})$ equals to the bias between the pre-measured step length and the average step length over this period, and random error $\tilde{\delta}^i_{k^i} = \delta^i_{k^i} - \mu^i_\delta$. We reasonably assume $\tilde{\delta}^i_k \sim N(0, \sigma^2_{\delta^i})$. Same as above, all the $\varphi^i_{k^i}$ are i.i.d.. $E(\varphi^i_{k^i}) = \mu^i_\varphi$ models the system bias of the movement direction measurement, such as the misalignment between the moving direction and the holding direction. $\tilde{\varphi}^i_{k^i} = \varphi^i_{k^i} - \mu^i_\varphi$ models the remaining random error, such as the direction error caused by hand shaking. We also assume $\tilde{\varphi}^i_{k^i} \sim N(0, \sigma^2_{\varphi^i})$. Then, the error can be divided into three parts:

$$\begin{aligned} e^i_{n^i} &\approx \sum_{k^i=1}^{n^i} (\tilde{\varphi}^i_{k^i} l^i_{k^i} \sin\theta^i_{k^i} - \tilde{\delta}^i_{k^i} \cos\theta^i_{k^i} + \mu^i_\varphi l^i_{k^i} \sin\theta^i_{k^i} - \mu^i_\delta \cos\theta^i_{k^i}) \\ &= \dot{e}^i_{n^i} - \mu^i_\delta \sum_{k^i=1}^{n^i} \cos\theta^i_{k^i} + \mu^i_\varphi \sum_{k^i=1}^{n^i} l^i_{k^i} \sin\theta^i_{k^i} = \dot{e}^i_{n^i} + \ddot{e}^i_{n^i} + \dddot{e}^i_{n^i}. \end{aligned}$$

From the property of normal distribution, $\dot{e}^i_{n^i} \sim N(0, \sigma^2_{\dot{e}^i_{n^i}})$. $\ddot{e}^i_{n^i}$ and $\dddot{e}^i_{n^i}$ are determined by how the pedestrian moves. They bring large bias during the movement. Adometer averages location estimates $\{x^j_{n^j}\}$ from M pedestrians, who meets each other at that second. The summation of errors has three parts $\sum_{j=1}^M e^j_{n^j} = \sum_{j=1}^M \dot{e}^j_{n^j} + \sum_{j=1}^M \ddot{e}^j_{n^j} + \sum_{j=1}^M \dddot{e}^j_{n^j}$.

The first part is random noise:

$$\sum_{i=1}^M \dot{e}^j_{n^j} \sim N(0, \sum_{j=1}^M \sigma^2_{\dot{e}^j_{n^j}}). \tag{5}$$

In the second part, $b^j_{n^j} = \sum_{k^j=1}^{n^j} \cos\theta^j_{k^j}$ is j's moving trace with uniform step length . It must satisfy the meeting constrain: $x_M - x^j_0 = \sum_{k^j=1}^{n^j} l^j_{k^j} \cos\theta^j_{k^j}$, where x_M is the meeting location. Notice that $b^j_{n^j} \approx x_M - x^j_0$ follows a discrete distribution, which mainly depends on the location and traffic of each entrance. In (1), we have $\mu^j_\delta \sim N(0, \sigma^2_{\mu_\delta})$. Because each pedestrian chooses the entrance randomly, μ^j_δ and $b^j_{n^j}$ are independent. Therefore, $\ddot{e}^j_{n^j} = \mu^j_\delta b^j_{n^j}$ are i.i.d. random variables with $E(\ddot{e}^j_{n^j}) = E(\mu^j_\delta b^j_{n^j}) = 0$ and $Var(\ddot{e}^j_{n^j}) = E({\mu^j_\delta}^2) E({b^j_{n^j}}^2) = \sigma^2_{\mu_\delta} E({b^j_{n^j}}^2)$. When $E({b^j_{n^j}}^2) \neq 0$ and M is large enough, the central limited theorem says that the approximate distribution is:

$$\sum_{j=1}^M \ddot{e}^j_{n^j} \sim N(0, \sum_{j=1}^M \sigma^2_{\mu_\delta} E({b^j_{n^j}}^2)). \tag{6}$$

Similar to the second part, $\sigma^2_{\mu_\varphi}$ is the variance of the distribution of μ^j_φ. $c^j_{n^j}$ is the abbreviation for $\sum_{k^j=1}^{n^j} l^j_{k^j} \sin\theta^j_{k^j}$.

$$\sum_{j=1}^M \dddot{e}^j_{n^j} \sim N(0, \sum_{j=1}^M \sigma^2_{\mu_\varphi} E({c^j_{n^j}}^2)). \tag{7}$$

From (5)(6)(7), the average gives error:

$$\bar{e}_M = \frac{\sum_{j=1}^M e^j_{n_j}}{M} \sim N(0, \sigma^2_{\bar{e}_M}) = N\Big(0, \frac{\sum_{j=1}^M \left(\sigma^2_{\dot{e}^j_{n^j}} + \sigma^2_{\mu_\delta} E({b^j_{n^j}}^2) + \sigma^2_{\mu_\varphi} E({c^j_{n^j}}^2)\right)}{M^2}\Big). \tag{8}$$

Through averaging, (a) the variance of random error $\dot{e}^j_{n^j}$ is reduced to $1/M$ of the origin value on average. (b) The bias error $\ddot{e}^j_{n^j}$ and $\dddot{e}^j_{n^j}$, are bounded by an unbiased normal distribution.

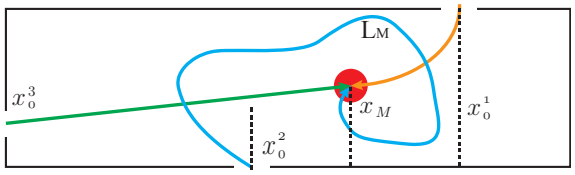

Fig. 11. Location Constraint